Stable $\mathcal{H}_2$-optimal controller synthesis

Joseph R. Corrado[1,†], R. Scott Erwin[2,‡], Dennis S. Bernstein[3,§]
and Wassim M. Haddad[4,*,‖]

[1]*School of Aerospace Engineering, Georgia Institute of Technology, Atlanta, GA 30332-0150, U.S.A.*
[2]*U.S. Air Force Research Laboratory, AFRL/VSDV, Building 472, 3550 Kirkland AFB, NM 87117-5776, U.S.A.*
[3]*Department of Aerospace Engineering, The University of Michigan, Ann Arbor, MI 48109-2118, U.S.A.*
[4]*School of Aerospace Engineering, Georgia Institute of Technology, Atlanta, GA 30332-0150, U.S.A.*

SUMMARY

This paper considers fixed-structure stable $\mathcal{H}_2$-optimal controller synthesis using a multiobjective optimization technique which provides a trade-off between closed-loop performance and the degree of controller stability. The problem is presented in a decentralized static output feedback framework developed for fixed-structure dynamic controller synthesis. A quasi-Newton/continuation algorithm is used to compute solutions to the necessary conditions. To demonstrate the approach, two numerical examples are considered. The first example is a second-order spring–mass–damper system and the second example is a fourth-order two-mass system, both of which are considered in the stable stabilization literature. The results are then compared with other methods of stable compensator synthesis. Copyright © 2000 John Wiley & Sons, Ltd.

KEY WORDS: Strong stabilization; fixed-order control; $\mathcal{H}_2$-optimal control

1. INTRODUCTION

It is well known that LQG synthesis can produce unstable (albeit stabilizing) controllers, especially at high authority levels. Of course, for certain plants, specifically those that do not satisfy the parity interlacing property [1], only unstable controllers are stabilizing. However, even

for stable plants, LQG often produces unstable controllers, thus requiring Nyquist encirclements of the critical point. However, these encirclements and the resulting multiple gain margins, which must be maintained by the input actuators, can be jeopardized by actuator saturation and startup dynamics [2]. Therefore, whenever possible, it is desirable to implement only stable controllers.

Several modifications of LQG theory have been proposed to obtain stable compensators. Several of these techniques involve either modified Riccati equations [3–5] or constrained weights [6, 7]. Thus the resulting controllers may sacrifice performance for controller stability. In [8, 9], an augmented cost technique related to the one used in this paper was proposed to obtain stable controllers without unnecessarily sacrificing performance. However, these papers focus on multiple-model control, and therefore the cost function to be optimized is a weighted average of a number of system costs and does not give any insight into the trade-off between system performance and controller stability margin.

The purpose of this paper is to provide a control-system design framework for $\mathcal{H}_2$-optimal strong stabilization. To achieve this goal we formulate the stable LQG problem within the context of decentralized static output feedback control which provides a general framework for fixed-structure dynamic controller synthesis [10, 11]. In particular, in order to guarantee stable stabilization, a multiobjective problem, reminiscent of scalarization techniques for Pareto optimization, is treated by forming a convex combination of the $\mathcal{H}_2$ norm of the closed-loop system and a weighted $\mathcal{H}_2$ norm of the controller. It is shown that as the trade-off parameter is varied to obtain better $\mathcal{H}_2$ system performance, the controller eigenvalues approach the imaginary axis. Thus, the control engineer can decide if additional performance improvements warrant the resulting reduction in the stability margin of the controller.

Two examples from the stable stabilization literature are considered in this paper. The first example is a second-order, spring–mass–damper system and the second example is a fourth-order, two-mass system involving two flexible modes. The $\mathcal{H}_2$ cost of the stable controllers developed for the first example, though larger than that of the LQG controller, was comparable to the lowest cost possible by a stable controller. For the second example, the difference between the $\mathcal{H}_2$ cost of the stable controller and the unstable LQG controller is negligible.

Finally, in this paper we use the following standard notation. Let $\mathbb{R}$ denote the set of real numbers, let $\mathbb{R}^{n \times m}$ denote the set of real $n \times m$ matrices, let $\mathbb{E}$ denote expectation, and let I_n denote the $n \times n$ identity matrix.

2. STABLE $\mathcal{H}_2$-OPTIMAL CONTROL

In this section we state the $\mathcal{H}_2$-optimal stable stabilization problem. Specifically, given the nth-order plant

$$\dot{x}(t) = Ax(t) + Bu(t) + D_1 w(t), \quad t \in [0, \infty) \tag{1}$$

with noisy measurements

$$y(t) = Cx(t) + Du(t) + D_2 w(t) \tag{2}$$

and performance variables

$$z(t) = E_1 x(t) + E_2 u(t) \tag{3}$$

where $u(t) \in \mathbb{R}^m$, $y(t) \in \mathbb{R}^l$, $z(t) \in \mathbb{R}^p$, and $w(t) \in \mathbb{R}^d$, and where $w(t)$ is a unit-intensity, zero-mean, Gaussian white noise signal, determine an n_c^{th}-order strictly proper dynamic compensator

$$\dot{x}_c(t) = A_c x_c(t) + B_c y(t) \tag{4}$$

$$u(t) = C_c x_c(t) \tag{5}$$

such that the $\mathcal{H}_2$ performance criterion

$$J(A_c, B_c, C_c) \triangleq \lim_{t \to \infty} \frac{1}{t} \mathbb{E} \int_0^t z^T(s) z(s) \, \mathrm{d}s \tag{6}$$

is minimized and the compensator dynamics matrix A_c is asymptotically stable.

The closed-loop system (1)–(5) is given by

$$\dot{\tilde{x}}(t) = \tilde{A}\tilde{x}(t) + \tilde{D}w(t), \quad t \in [0, \infty) \tag{7}$$

$$z(t) = \tilde{E}\tilde{x}(t) \tag{8}$$

where

$$\tilde{x}(t) \triangleq \begin{bmatrix} x(t) \\ x_c(t) \end{bmatrix}, \quad \tilde{A} \triangleq \begin{bmatrix} A & BC_c \\ B_c C & A_c + B_c DC_c \end{bmatrix}, \quad \tilde{D} \triangleq \begin{bmatrix} D_1 \\ B_c D_2 \end{bmatrix}, \quad \tilde{E} \triangleq \begin{bmatrix} E_1 & E_2 C_c \end{bmatrix}$$

and where the closed-loop disturbance $\tilde{D}w(t)$ has intensity

$$\tilde{V} \triangleq \tilde{D}\tilde{D}^T = \begin{bmatrix} V_1 & 0 \\ 0 & B_c V_2 B_c^T \end{bmatrix} \tag{9}$$

where $V_1 \triangleq D_1 D_1^T$, $V_2 \triangleq D_2 D_2^T$, and $V_{12} \triangleq D_1 D_2^T = 0$. The closed-loop transfer function from disturbances w to performance variables z is given by

$$G_{zw}(s) \triangleq \tilde{E}(sI_{\tilde{n}} - \tilde{A})^{-1} \tilde{D}$$

where $\tilde{n} \triangleq n + n_c$. Next, define a weighted controller transfer function from plant output y to plant input u by

$$\hat{G}_c(s) \triangleq E_2 C_c (sI_{n_c} - A_c)^{-1} B_c D_2$$

Hence, the fixed-structure stable $\mathscr{H}_2$-optimal control problem is defined as:

$$\min_{(A_c, B_c, C_c)} \|G_{zw}(s)\|_2^2$$

subject to

$$\|\hat{G}_c(s)\|_2^2 < \infty$$

3. DECENTRALIZED STATIC OUTPUT FEEDBACK FRAMEWORK

In this section we use the fixed-structure control framework given in [10, 11] to transform the $\mathscr{H}_2$-optimal stable stabilization problem to a decentralized static output feedback setting. Consider the 4-vector input–4-vector output decentralized system shown in Figure 1, where $\hat{G}(s)$ represents the linear, time-invariant dynamical system

$$\dot{\tilde{x}}(t) = \mathscr{A}\tilde{x}(t) + \sum_{i=1}^{3} \mathscr{B}_{ui}u_i(t) + \mathscr{B}_w w(t), \quad t \in [0, \infty) \tag{10}$$

$$y_i(t) = \mathscr{C}_{yi}\tilde{x}(t) + \mathscr{D}_{yw_i}w(t), \quad i = 1, 2, 3 \tag{11}$$

$$z(t) = \mathscr{C}_z\tilde{x}(t) + \sum_{i=1}^{3} \mathscr{D}_{zu_i}u_i(t) \tag{12}$$

where

$$u_1(t) = A_c y_1(t), \quad u_2(t) = B_c y_2(t), \quad u_3(t) = C_c y_3(t) \tag{13}$$

and

$$\mathscr{A} \triangleq \begin{bmatrix} A & 0 \\ 0 & 0 \end{bmatrix}, \qquad \mathscr{B}_w \triangleq \begin{bmatrix} D_1 \\ 0 \end{bmatrix}, \qquad \mathscr{C}_z \triangleq \begin{bmatrix} E_1 & 0 \end{bmatrix}$$

$$\mathscr{B}_{u_1} \triangleq \begin{bmatrix} 0 \\ I_{n_c} \end{bmatrix}, \qquad \mathscr{B}_{u_2} \triangleq \begin{bmatrix} 0 \\ I_{n_c} \end{bmatrix}, \qquad \mathscr{B}_{u_3} \triangleq \begin{bmatrix} B \\ 0 \end{bmatrix}$$

$$\mathscr{C}_{y_1} \triangleq \begin{bmatrix} 0 & I_{n_c} \end{bmatrix}, \qquad \mathscr{C}_{y_2} \triangleq \begin{bmatrix} C & 0 \end{bmatrix}, \qquad \mathscr{C}_{y_3} \triangleq \begin{bmatrix} 0 & I_{n_c} \end{bmatrix}$$

$$\mathscr{D}_{yw_1} \triangleq 0, \qquad \mathscr{D}_{yw_2} \triangleq D_2, \qquad \mathscr{D}_{yw_3} \triangleq 0$$

$$\mathscr{D}_{zu_1} \triangleq 0, \qquad \mathscr{D}_{zu_2} \triangleq 0, \qquad \mathscr{D}_{zu_3} \triangleq E_2$$
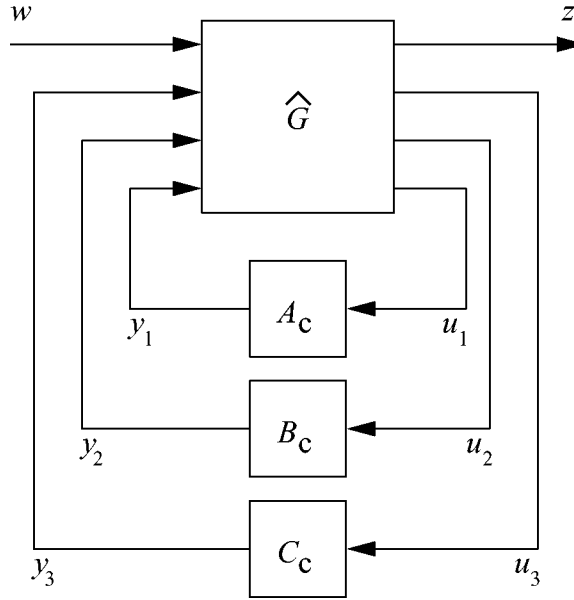
Figure 1. Decentralized static output feedback framework.

Next, defining

$$\hat{u}(t) \triangleq \begin{bmatrix} u_1(t) \\ u_2(t) \\ u_3(t) \end{bmatrix}, \qquad \hat{y}(t) \triangleq \begin{bmatrix} y_1(t) \\ y_2(t) \\ y_3(t) \end{bmatrix}$$

$$\mathcal{B}_u \triangleq \begin{bmatrix} \mathcal{B}_{u_1} & \mathcal{B}_{u_2} & \mathcal{B}_{u_3} \end{bmatrix}, \qquad \mathcal{D}_{zu} \triangleq \begin{bmatrix} \mathcal{D}_{zu_1} & \mathcal{D}_{zu_2} & \mathcal{D}_{zu_3} \end{bmatrix}$$

$$\mathcal{C}_y \triangleq \begin{bmatrix} \mathcal{C}_{y_1} \\ \mathcal{C}_{y_2} \\ \mathcal{C}_{y_3} \end{bmatrix}, \qquad \mathcal{D}_{yw} \triangleq \begin{bmatrix} \mathcal{D}_{yw_1} \\ \mathcal{D}_{yw_2} \\ \mathcal{D}_{yw_3} \end{bmatrix}$$

and rewriting the decentralized control signals (13) in the compact form

$$\hat{u}(t) = \mathcal{K}\hat{y}(t) \tag{14}$$

where

$$\mathcal{K} \triangleq \begin{bmatrix} A_c & 0 & 0 \\ 0 & B_c & 0 \\ 0 & 0 & C_c \end{bmatrix}$$

the closed-loop dynamics

$$\dot{\tilde{x}}(t) = \tilde{A}\tilde{x}(t) + \tilde{D}w(t), \quad t \in [0, \infty) \tag{15}$$

$$z(t) = \tilde{E}\tilde{x}(t) \tag{16}$$

are identical to (7) and (8), but now $\tilde{A}$, $\tilde{D}$, and $\tilde{E}$ can be written as

$$\tilde{A} = \mathscr{A} + \mathscr{B}_u \mathscr{K} \mathscr{C}_y, \quad \tilde{D} = \mathscr{B}_w + \mathscr{B}_u \mathscr{K} \mathscr{D}_{yw}, \quad \tilde{E} = \mathscr{C}_z + \mathscr{D}_{zu} \mathscr{K} \mathscr{C}_y.$$

The $\mathscr{H}_2$ norm of $G_{zw}(s)$ is given by

$$\|G_{zw}(s)\|_2^2 = \operatorname{tr} \tilde{Q}\tilde{R} \tag{17}$$

where $\tilde{Q}$ is the unique, $\tilde{n} \times \tilde{n}$ non-negative-definite solution to the algebraic Lyapunov equation

$$0 = \tilde{A}\tilde{Q} + \tilde{Q}\tilde{A}^\mathrm{T} + \tilde{D}\tilde{D}^\mathrm{T} \tag{18}$$

and where

$$\tilde{R} \triangleq \tilde{E}^\mathrm{T}\tilde{E} = \begin{bmatrix} R_1 & 0 \\ 0 & C_\mathrm{c}^\mathrm{T}R_2 C_\mathrm{c} \end{bmatrix} \tag{19}$$

where $R_1 \triangleq E_1^\mathrm{T}E_1$, $R_2 \triangleq E_2^\mathrm{T}E_2$, and $R_{12} \triangleq E_1^\mathrm{T}E_2 = 0$. Furthermore, if A_c is stable, then the $\mathscr{H}_2$ norm of the weighted transfer function of the controller $\hat{G}_\mathrm{c}(s) = E_2 C_\mathrm{c}(sI_{n_\mathrm{c}} - A_\mathrm{c})^{-1}B_\mathrm{c}D_2$ is given by

$$\|\hat{G}_\mathrm{c}(s)\|_2^2 = \operatorname{tr} Q_\mathrm{c} C_\mathrm{c}^\mathrm{T}R_2 C_\mathrm{c} \tag{20}$$

where Q_c is the unique, $n_\mathrm{c} \times n_\mathrm{c}$ nonnegative-definite solution to the algebraic Lyapunov equation

$$0 = A_\mathrm{c}Q_\mathrm{c} + Q_\mathrm{c}A_\mathrm{c}^\mathrm{T} + B_\mathrm{c}V_2 B_\mathrm{c}^\mathrm{T} \tag{21}$$

To obtain (20) and (21) in terms of $\mathscr{K}$, we define the matrices

$$L_{A_\mathrm{c}} \triangleq [I_{n_\mathrm{c}} \quad 0 \quad 0], \qquad R_{A_\mathrm{c}} \triangleq \begin{bmatrix} I_{n_\mathrm{c}} \\ 0 \\ 0 \end{bmatrix}$$

$$L_{B_\mathrm{c}} \triangleq [0 \quad I_{n_\mathrm{c}} \quad 0], \qquad R_{B_\mathrm{c}} \triangleq \begin{bmatrix} 0 \\ I_l \\ 0 \end{bmatrix}$$

$$L_{C_c} \triangleq [0 \quad 0 \quad I_m], \qquad R_{C_c} \triangleq \begin{bmatrix} 0 \\ 0 \\ I_{n_c} \end{bmatrix}$$

so that $L_{A_c} \mathscr{K} R_{A_c} = A_c$, $L_{B_c} \mathscr{K} R_{B_c} = B_c$, and $L_{C_c} \mathscr{K} R_{C_c} = C_c$. Thus, (20) and (21) become

$$\|\hat{G}_c(s)\|_2^2 = \text{tr } Q_c R_{C_c}^{\mathrm{T}} \mathscr{K}^{\mathrm{T}} L_{C_c}^{\mathrm{T}} R_2 L_{C_c} \mathscr{K} R_{C_c} \tag{22}$$

and

$$0 = L_{A_c} \mathscr{K} R_{A_c} Q_c + Q_c R_{A_c}^{\mathrm{T}} \mathscr{K}^{\mathrm{T}} L_{A_c}^{\mathrm{T}} + L_{B_c} \mathscr{K} R_{B_c} V_2 R_{B_c}^{\mathrm{T}} \mathscr{K}^{\mathrm{T}} L_{B_c}^{\mathrm{T}} \tag{23}$$

respectively.

In order to design stable $\mathscr{H}_2$-optimal controllers we pose the following multiobjective optimization problem: For $\rho \in [0, 1]$, determine $\mathscr{K}$ that minimizes:

$$\mathscr{J}(\mathscr{K}) = (1 - \rho) \text{ tr } \tilde{Q}\tilde{R} + \rho \text{ tr } Q_c R_{C_c}^{\mathrm{T}} \mathscr{K}^{\mathrm{T}} L_{C_c}^{\mathrm{T}} R_2 L_{C_c} \mathscr{K} R_{C_c} \tag{24}$$

where $\tilde{Q}, Q_c \geq 0$ satisfy (18) and (23), respectively. Note that (24) involves a convex combination of the $\mathscr{H}_2$ closed-loop system norm and the weighted $\mathscr{H}_2$ norm of the controller, varied with the trade-off parameter ρ. By including the $\mathscr{H}_2$ cost of the controller in the objective function, we can guarantee that the controller is stable as long as the objective function is finite. By varying $\rho \in [0, 1]$, (24) can be viewed as the scalar representation of a multiobjective cost. To achieve the best closed-loop performance with a stable controller, we only want to use the $\mathscr{H}_2$ cost of the controller as a constraint, and thus we set $\rho > 0$ to be small so that the $\mathscr{H}_2$ cost of the controller is negligible compared to the $\mathscr{H}_2$ cost of the closed-loop system. By doing this, the optimization routine will minimize the cost of the closed-loop system, and not attempt to minimize the $\mathscr{H}_2$ cost of the compensator. However, increasing the size of the trade-off parameter ρ will increase the controller stability margin. Finally, note that by letting $\rho \to 0$, we recover the $\mathscr{H}_2$-optimal control problem.

The necessary conditions for optimality can be derived by forming the Lagrangian

$$\mathscr{L}(\tilde{P}, \tilde{Q}, P_c, Q_c, \mathscr{K}) = (1 - \rho) \text{ tr } \tilde{Q}\tilde{R} + \text{tr } \tilde{P}[\tilde{A}\tilde{Q} + \tilde{Q}\tilde{A}^{\mathrm{T}} + \tilde{V}]$$

$$+ \rho \text{ tr } Q_c R_{C_c}^{\mathrm{T}} \mathscr{K}^{\mathrm{T}} L_{C_c}^{\mathrm{T}} R_2 L_{C_c} \mathscr{K} R_{C_c} + \text{tr } P_c [L_{A_c} \mathscr{K} R_{A_c} Q_c + Q_c R_{A_c}^{\mathrm{T}} \mathscr{K}^{\mathrm{T}} L_{A_c}^{\mathrm{T}}$$

$$+ L_{B_c} \mathscr{K} R_{B_c} V_2 R_{B_c}^{\mathrm{T}} \mathscr{K}^{\mathrm{T}} L_{B_c}^{\mathrm{T}}] \tag{25}$$

where $\tilde{P} \in \mathbb{R}^{\tilde{n} \times \tilde{n}}$ and $P_c \in \mathbb{R}^{n_c \times n_c}$ are Lagrange multipliers. The partial derivatives with respect to the free parameters in (25) are given by

$$\frac{\partial \mathscr{L}}{\partial \tilde{Q}} = \tilde{A}^{\mathrm{T}}\tilde{P} + \tilde{P}\tilde{A} + (1 - \rho)\tilde{R}$$

$$\frac{\partial \mathscr{L}}{\partial \tilde{P}} = \tilde{A}\tilde{Q} + \tilde{Q}\tilde{A}^{\mathrm{T}} + \tilde{V}$$

$$\frac{\partial \mathscr{L}}{\partial Q_{\mathrm{c}}} = A_{\mathrm{c}}^{\mathrm{T}}P_{\mathrm{c}} + P_{\mathrm{c}}A_{\mathrm{c}} + \rho C_{\mathrm{c}}^{\mathrm{T}}R_2 C_{\mathrm{c}}$$

$$\frac{\partial \mathscr{L}}{\partial P_{\mathrm{c}}} = A_{\mathrm{c}}Q_{\mathrm{c}} + Q_{\mathrm{c}}A_{\mathrm{c}}^{\mathrm{T}} + B_{\mathrm{c}}V_2 B_{\mathrm{c}}^{\mathrm{T}}$$

$$\frac{\partial \mathscr{L}}{\partial A_{\mathrm{c}}} = L_{A_{\mathrm{c}}}\frac{\partial \mathscr{L}}{\partial \mathscr{K}}R_{A_{\mathrm{c}}}, \quad \frac{\partial \mathscr{L}}{\partial B_{\mathrm{c}}} = L_{B_{\mathrm{c}}}\frac{\partial \mathscr{L}}{\partial \mathscr{K}}R_{B_{\mathrm{c}}}, \quad \frac{\partial \mathscr{L}}{\partial C_{\mathrm{c}}} = L_{C_{\mathrm{c}}}\frac{\partial \mathscr{L}}{\partial \mathscr{K}}R_{C_{\mathrm{c}}}$$

where

$$\frac{\partial \mathscr{L}}{\partial \mathscr{K}} = \mathscr{B}_u^{\mathrm{T}}\tilde{P}\tilde{Q}\mathscr{C}_y^{\mathrm{T}} + \mathscr{B}_u^{\mathrm{T}}\tilde{P}\tilde{V}\mathscr{D}_{yw}^{\mathrm{T}} + (1-\rho)\mathscr{D}_{zu}^{\mathrm{T}}\tilde{E}\tilde{Q}\mathscr{C}_y^{\mathrm{T}}$$

$$+ \rho L_{C_{\mathrm{c}}}^{\mathrm{T}}R_2 L_{C_{\mathrm{c}}}\mathscr{K}R_{C_{\mathrm{c}}}Q_{\mathrm{c}}R_{C_{\mathrm{c}}}^{\mathrm{T}} + L_{A_{\mathrm{c}}}^{\mathrm{T}}P_{\mathrm{c}}Q_{\mathrm{c}}R_{A_{\mathrm{c}}}^{\mathrm{T}} + L_{B_{\mathrm{c}}}^{\mathrm{T}}L_{B_{\mathrm{c}}}\mathscr{K}R_{B_{\mathrm{c}}}V_2 R_{B_{\mathrm{c}}}^{\mathrm{T}}$$

4. QUASI-NEWTON/CONTINUATION ALGORITHM

To solve the non-linear optimization problem posed in Section 3, a general-purpose BFGS quasi-Newton algorithm [12] is used. The line-search portions of the algorithm were modified to include a constraint-checking subroutine to verify the search direction vector lies entirely within the set of parameters that yield a stable closed-loop system. This modification ensures that the cost function $\mathscr{J}$ remains defined at every point in the line-search process.

One requirement of gradient-based optimization algorithms is an initial stabilizing design. For plants satisfying the parity interlacing property, initialization can be accomplished by using sufficiently low authority compensators [13]. This was accomplished here by multiplying the control weight E_2 by a scalar $\eta > 1$. At sufficiently low authority, the LQG controllers were stable. These low authority, stable, full-order controllers can generally be truncated using an appropriate model reduction technique without destroying closed-loop stability. For decentralized control, this technique can be implemented in a sequential manner for each channel to obtain initializing gains with the given structure. These low authority LQG designs are used to initialize a low authority optimization algorithm. The optimized controller gains are then used to sequentially initialize higher authority problems until eventually the desired high authority design is obtained. When the required authority is regained, the trade-off parameter ρ is varied until the best $\mathscr{H}_2$ performance is attained in the face of a desired controller stability margin.

Finally, we note that the optimization problem described above is non-convex. This makes complexity analysis extremely difficult since complexity results are developed almost exclusively for convex optimization problems. However, the lack of convexity here is not simply a limitation of the stable stabilization formulation since the reduced-order control design problem is an inherently non-convex optimization problem.
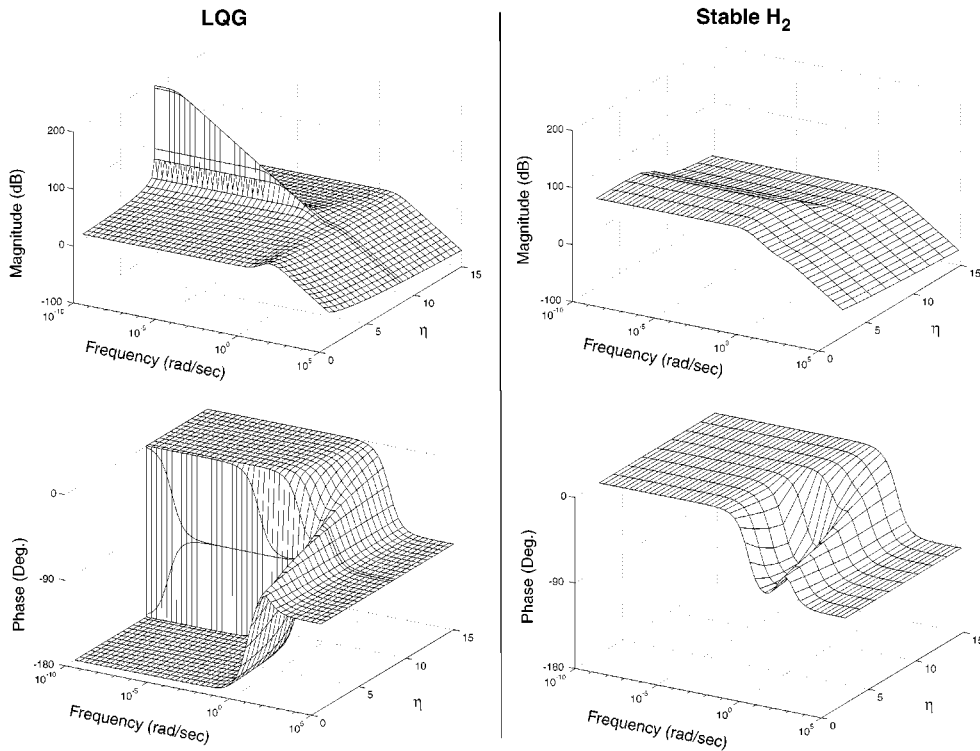
Figure 2. Bode plots of LQG and stable $\mathscr{H}_2$ controllers ($\rho = 0.0288$).

5. SPRING–MASS–DAMPER EXAMPLE

Consider the spring–mass–damper system given by the state-space realization [6, 14]

$$\dot{x}(t) = \begin{bmatrix} 0 & 1 \\ -3 & -4 \end{bmatrix} x(t) + \begin{bmatrix} 0 \\ 1 \end{bmatrix} u(t)$$

$$y(t) = \begin{bmatrix} 2 & 1 \end{bmatrix} x(t)$$

The matrices D_1, D_2, E_1, and E_2 are chosen to be

$$D_1 = \begin{bmatrix} 35 & 0 \\ -61 & 0 \end{bmatrix}, \quad D_2 = \begin{bmatrix} 0 & 1 \end{bmatrix}, \quad E_1 = \begin{bmatrix} 52.9150 & 8.9443 \\ 0 & 0 \end{bmatrix}, \quad E_2 = \begin{bmatrix} 0 \\ 1 \end{bmatrix}$$

For the given data, the LQG controller is unstable. To initialize the stable $\mathscr{H}_2$-optimal control problem, the control weighting was increased by multiplying E_2 by $\eta = 16$, as described in Section 4. This stable LQG design was used as a starting point for the quasi-Newton algorithm which found optimal stable compensators as η was decremented back to unity, returning the control authority to its original value.
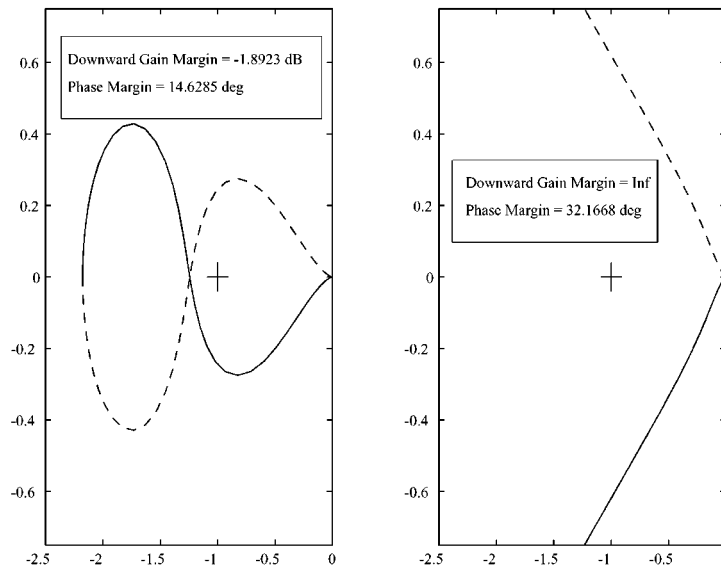
Figure 3. Nyquist plots of the loop gain for LQG and stable $\mathscr{H}_2$ controllers ($\rho = 0.0288$).

As can be seen in Figure 2, increasing the authority toward a critical level ($\eta = 8.58$) causes the gain of the LQG controller to approach infinity, at which point the low-frequency phase jumps $-180°$ and the gain begins to decrease, though the controller must now be unstable to maintain closed-loop stability. At this point, it can be seen that the magnitude of the stable $\mathscr{H}_2$-optimal controllers increase as well, though not as drastically as the LQG design, and the stable $\mathscr{H}_2$-optimal controllers always have a phase of $0°$ at low frequencies. The Nyquist plots of the LQG controller and the stable controller at full control authority, as seen in Figure 3, show the poor gain margins of the unstable LQG controller.

Since the loop gain with the $\mathscr{H}_2$-optimal stable controller in feedback is much larger than that with the LQG controller at full authority, the impulse responses of the LQG and the stable controllers were simulated to compare the actual controller efforts needed to bring the closed-loop system back to the equilibrium. These comparisons are shown in Figure 4. As expected, the performance of the system with the LQG controller is better than the performance of the system with the stable $\mathscr{H}_2$-optimal controller. However, note that even though the loop gain of the stable controller is much larger than that of the LQG controller, the control effort used by the stable controller is significantly less than that used by the LQG controller and hence is less likely to saturate the system actuators, which could cause closed-loop instabilities to occur when an unstable controller is used.

Once the control authority was increased to the desired level, the value of the parameter ρ was varied to study the trade-off between the $\mathscr{H}_2$ cost of the system and the stability level of the compensator. Figure 5 shows the position of the controller ($n_c = 2$) eigenvalues as a function of ρ as well as the $\mathscr{H}_2$ cost of the closed-loop system as a function of ρ. By studying the resulting trade-off, the control engineer can decide if subsequent cost reductions justify bringing the controller eigenvalues closer to the stability boundary.
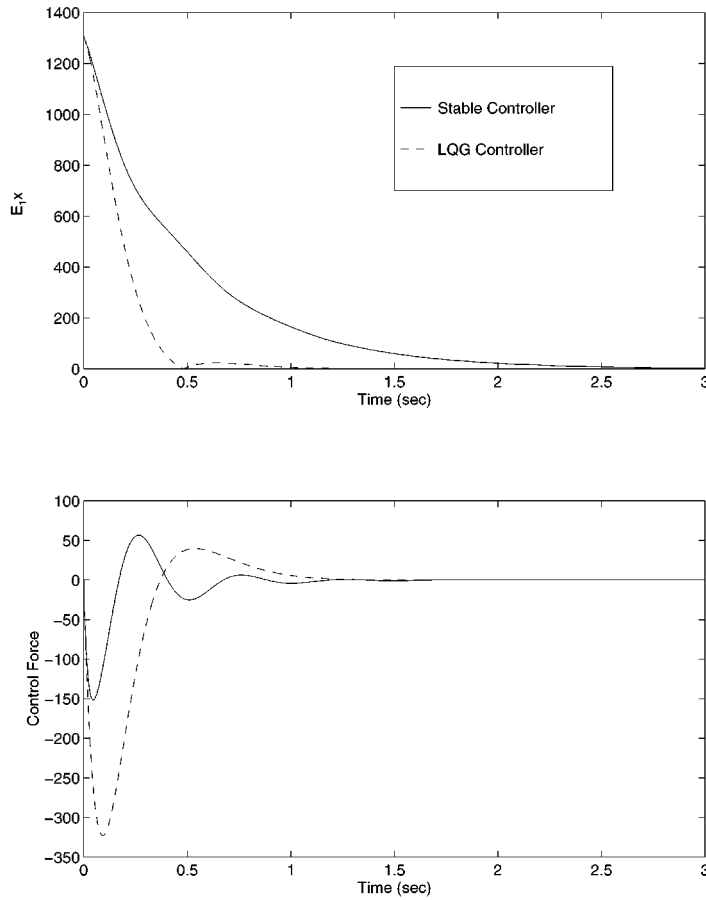
Figure 4. Impulse response of closed-loop system with LQG and stable $\mathcal{H}_2$ controllers ($\eta = 1$, $\rho = 2.88 \times 10^{-8}$).

For $\rho = 0.5$, the controller transfer function is given by

$$G_c(s) = \frac{-274.21s - 4183.8}{s^2 + 38.324s + 43.539} \tag{26}$$

which has eigenvalues at $\lambda_1 = -37.152$ and $\lambda_2 = -1.1719$, while, for $\rho = 5 \times 10^{-7}$, the controller transfer function is given by

$$G_c(s) = \frac{-504.93s - 9744.5}{s^2 + 60.543s + 0.086523} \tag{27}$$

which has eigenvalues at $\lambda_1 = -60.541$ and $\lambda_2 = -0.0014292$.

Figure 5. Location of controller eigenvalues and $\mathscr{H}_2$ cost versus ρ.

Since, as stated in [14], the lowest possible cost via stable stabilization for this example is given by a fourth-order controller we used the present framework to obtain stable fourth-, sixth-, and eighth-order controllers to quantify the benefits of expanded-order control. Specifically, these expanded-order stable $\mathscr{H}_2$-optimal controllers were initialized by adding one, two, and three stable modes to a full-order stable LQG controller, at which point the optimization algorithm was applied. The corresponding closed-loop costs, computed at various levels of control authority, are shown in Figure 6. At lower levels of controller authority, the stable controllers have nearly identical costs to the LQG controllers. As the authority is increased, the closed-loop cost associated with the stable controllers becomes noticeably worse than the LQG controllers, however it is noticeably better than the best LQG design with a stable controller (i.e., the LQG design with $\eta = 8.58$). At the specified control authority ($\eta = 1$), the dependence of the augmented cost function on the controller cost was decreased by decreasing the variable ρ.

As seen in Figure 7, the full-order controller has the highest $\mathscr{H}_2$ cost, followed by the controller with one extra mode. The other two controllers, however, have nearly identical closed-loop costs, suggesting that arbitrarily high-order controllers may not achieve significant performance improvements. Since decreasing ρ decreases the dependence of the cost function J on the weighted $\mathscr{H}_2$ cost of the controller, the controller loop gain increases greatly as ρ becomes smaller, as shown in Figure 8.

Table I shows that the stable $\mathscr{H}_2$-optimal controllers obtained here compare favourably to earlier results. In [6], the design weights were constrained in such a way as to yield stable controllers. Even with a tuning procedure, however, those costs are larger than what was obtained using the present framework. In [14], a non-linear programming approach was used to obtain $\mathscr{H}_2$-optimal controllers, but only for SISO systems. However, as can be seen,
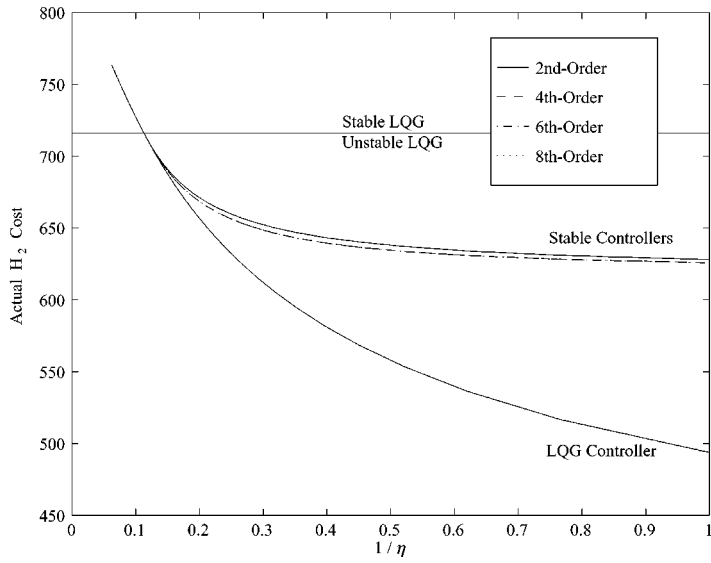
Figure 6. $\mathscr{H}_2$ cost versus control weighting for various-order stable $\mathscr{H}_2$ controllers ($\rho = 0.0288$).
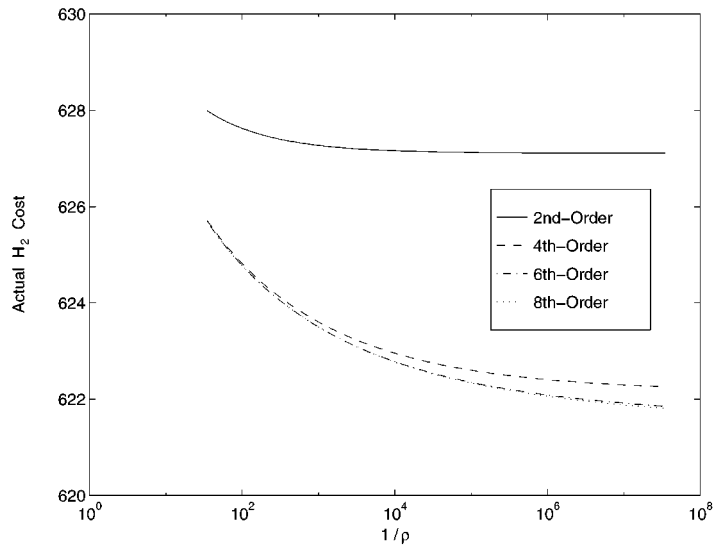

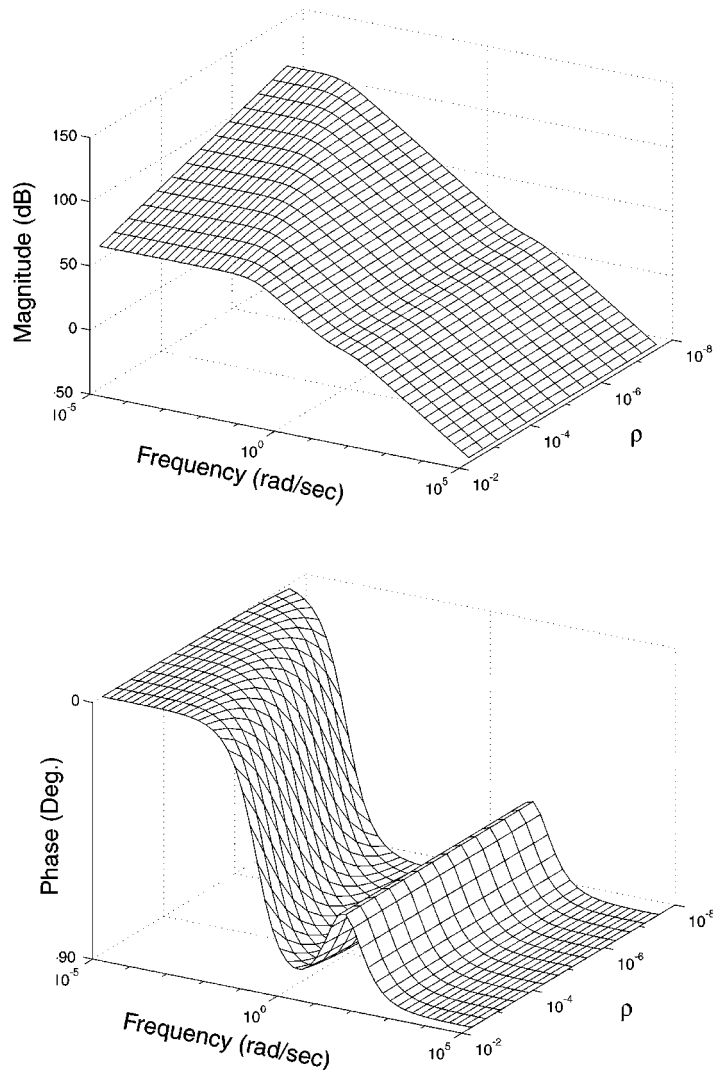Figure 7. Stable $\mathscr{H}_2$ controller cost versus ρ.

Figure 8. Bode plots of stable $\mathscr{H}_2$ controllers versus ρ.

the $\mathscr{H}_2$ cost is slightly larger than the fourth-order controllers designed here. In fact, the optimal controllers obtained in [14] had two poles located at the origin, and thus the controller was merely conditionally stable. The stability boundary was then pushed back to $s = -0.5$ to yield a stable controller. It should be noted that the cost obtained by the second-order controller synthesized using our method was 627.1, whereas in [9], it is stated that the minimum cost possible by a second-order stable compensator is 628, though this may be simply a numerical artifact. Also, listed is the $\mathscr{H}_2$ cost of an LQG design with η chosen as low as possible while still yielding a stable controller, which is significantly larger than all other methods considered.

Table I. $\mathcal{H}_2$ costs for various stable stabilization techniques.

	Second order	Fourth order	Sixth order	Eighth order
Fixed structure	627.11	622.20	621.73	621.67
Ganesh [14] (optimal)	N/A	622.73	N/A	N/A
Ganesh (sub-ptimal)	N/A	628.40	N/A	N/A
Halevi [6] (first result)	678.97	N/A	N/A	N/A
Halevi (after tuning)	637.18	N/A	N/A	N/A
Stable LQG ($\eta = 8.58$)	713.02	N/A	N/A	N/A

6. TWO-MASS EXAMPLE

Consider the dynamic system [4] shown in Figure 9. The equations of motion for this system are given by

$$m_1 \ddot{x}_1(t) + k(x_1(t) - x_2(t)) = u(t)$$

$$m_2 \ddot{x}_2(t) + k(x_2(t) - x_1(t)) = 0$$

Here we consider the case of a colocated sensor and actuator pair, where the output is given by $y = x_1$. Letting $m_1 = m_2 = k$ yields the plant state-space realization

$$\dot{x}(t) = \begin{bmatrix} 0 & 0 & 1 & 0 \\ 0 & 0 & 0 & 1 \\ -1 & 1 & 0 & 0 \\ 1 & -1 & 0 & 0 \end{bmatrix} x(t) + \begin{bmatrix} 0 \\ 0 \\ 1 \\ 0 \end{bmatrix} u(t)$$

$$y(t) = \begin{bmatrix} 1 & 0 & 0 & 0 \end{bmatrix} x(t).$$

As in [4], the matrices D_1, D_2, E_1, and E_2 are chosen to be

$$D_1 = \begin{bmatrix} 0 & 0 \\ 0 & 0 \\ 0 & 0 \\ 68 & 0 \end{bmatrix}, \quad D_2 = \begin{bmatrix} 0 & 1 \end{bmatrix}, \quad E_1 = \begin{bmatrix} 1 & 0 & 1 & 0 \\ 0 & 0 & 0 & 0 \end{bmatrix}, \quad E_2 = \begin{bmatrix} 0 \\ 0.01 \end{bmatrix}.$$

For this example, a full-order and a reduced-order stable $\mathcal{H}_2$-optimal controller were developed. The control authority was chosen to be sufficiently low so that the LQG controller was stable. This controller was then used to initialize the optimization algorithm.

The same general trends can be observed here as in the first example, though in this case, even when full authority is achieved, the $\mathcal{H}_2$ cost of the full-order stable controller rivals the performance of the unstable $\mathcal{H}_2$-optimal LQG controller, which would be apparent in Figure 10 if the curves were not directly on each other. In fact, the relative difference in the $\mathcal{H}_2$ costs is
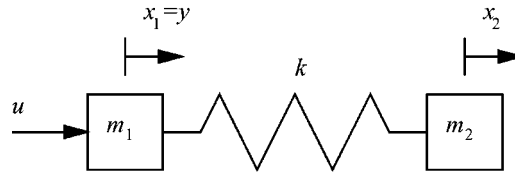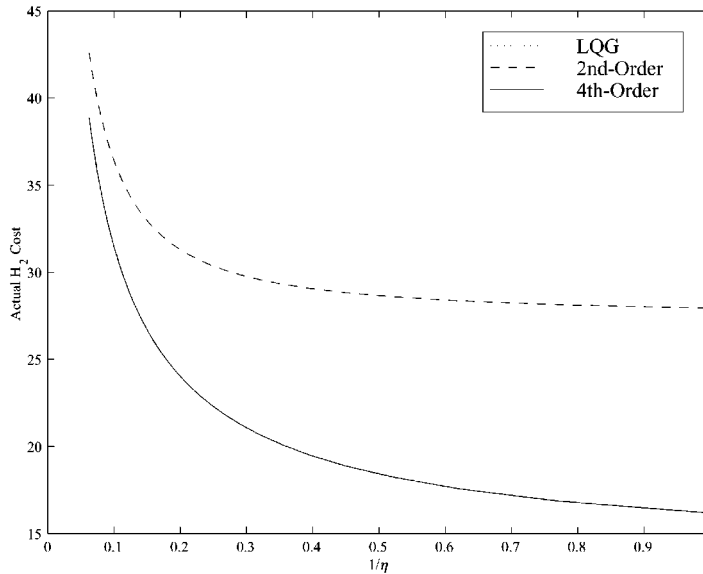
Figure 9. Two-mass system.

Figure 10. $\mathscr{H}_2$ cost versus control weighting ($\rho = 0.04752$).

merely 9.7114×10^{-4} per cent. For this reason, expanded-order controllers could not give further cost improvements to justify their increased complexity, and thus were not designed for this example. Also, the initial value of ρ was sufficiently small that further reductions did not improve the $\mathscr{H}_2$ cost of the closed-loop system. Table II compares the performance of the stable $\mathscr{H}_2$-optimal controller designs with LQG, stable LQG (LQG controller with η chosen as low as possible while still yielding a stable controller), and the full-order controller designed in [4], which used an over bounding approach along with parameter tunings to obtain stable controllers.

The ability of this stable controller to achieve an $\mathscr{H}_2$ performance nearly identical to that of the LQG controller was then explored. After running numerous examples, it appears that a minimum phase open-loop stable plant (such as the first example) will yield a significant performance degradation when the controller is constrained to be stable. However, a minimum phase, open-loop unstable plant does not seem to exhibit this lack of performance, as demonstrated by this example. Further investigation seems to show that stable $\mathscr{H}_2$-optimal

Table II. $\mathcal{H}_2$ costs for various stable stabilization techniques.

	Second order	Fourth order
LQG	N/A	16.175703
Fixed structure	27.9340	16.175782
Wang [4]	N/A	16.261138
Stable LQG ($\eta = 12.21$)	N/A	34.334324

controllers designed for non-minimum phase, open-loop unstable plants will also show performance degradation over an LQG controller, whereas no appreciable loss of performance occurred when a stable $\mathcal{H}_2$-optimal controller was designed for a non-minimum phase, open-loop stable plant.

7. DISCUSSION AND CONCLUSION

In this paper we investigated a scheme to synthesize $\mathcal{H}_2$-optimal controllers by including the $\mathcal{H}_2$ cost of the controller in the Lagrangian and using a multiobjective optimization technique. The problem was formulated in a decentralized static output feedback framework, which facilitated use of a quasi-Newton optimization algorithm. This technique was applied to two numerical examples. It was numerically shown that for some systems, namely minimum phase, open-loop unstable or non-minimum phase, open-loop stable plants, a stable controller can rival the performance of an unstable $\mathcal{H}_2$-optimal LQG controller and yet not be constrained by the loop margins of unstable controllers. For other systems, however, there could be a significant degradation in performance by requiring the controller to remain stable, although this technique provided controllers yielding the minimal $\mathcal{H}_2$ closed-loop cost for all stable linear controllers.

REFERENCES

1. Youla DC, Bongiorno JJ, Lu CN. Single loop feedback-stabilization of linear multivariable dynamical plants, *Automatica*, 1974; **10**: 159–173.
2. MacMartin DG, How JP. Implementation and prevention of unstable compensators, *Proceedings of the American Control Conference*, Baltimore, MD, June, 1994; 2190–2195.
3. Wang YW, Bernstein DS. $\mathcal{H}_2$-suboptimal stable stabilization. *Automatica*, 1994; **30**: 1797–1800.
4. Wang YW, Haddad WM, Bernstein DS. Stable stabilization with $\mathcal{H}_2$ and $\mathcal{H}_\infty$ performance constraints, *Journal of Mathematical Systems, Estimation, and Control*, 1996; **6**: 181–194.
5. Jacobus M, Jamshidi M, Abdallah C, Dorato P, Bernstein D. Suboptimal strong stabilization using fixed-order dynamic compensation, *Proceedings of the American Control Conference*, San Diego, CA, May, 1990; 2659–2660.
6. Halevi Y, Bernstein DS, Haddad WM. On stable full-order and reduced-order LQG controllers. *Optimal Control Application & Methods*, 1991, **12**: 163–172.

7. Halevi Y. Stable LQG controllers, *IEEE Transactions on Automatic Control*, 1994, **39**: 2104–2106.
8. MacMartin DG, Hall SR, Bernstein DS. Fixed-order multi-model estimation and control, *Proceedings of the American Control Conference*, Boston, MA, June, 1991; 2113–2118.
9. Grocott SCO, MacMartin DG, Miller DW. Experimental implementation of a multi-model design technique for robust control of the MACE test article, *Proceedings of the Third International Conference Adaptive Structures*, San Diego, CA, November, 1992; 375–387.
10. Bernstein DS, Haddad WM, Nett CN. Minimal complexity control law synthesis, part 2: problem solution via $\mathcal{H}_2/\mathcal{H}_\infty$ optimal static output feedback, *Proceedings of the American Control Conference*, Pittsburgh, PA, June, 1989, 2506–2511, also appears in *Recent Advances in Robust Control*, Dorato P, Yedavalli RK (eds.). IEEE Press: New York, 1990; 288–293.
11. Erwin RS, Sparks AG, Bernstein DS. Decentralized real structured singular value synthesis, *Proceedings of the 13th IFAC World Congress*, vol. C; Control Design I, San Francisco, CA, July 1996; 79–84.
12. Dennis Jr. JE, Schnabel RB. *Numerical Methods for Unconstrained Optimization and Nonlinear Equations*, Prentice-Hall, Englewood Cliffs, NJ, 1983.
13. Collins Jr. EG, Haddad WM, Ying SS. Construction of low-authority, nearly non-minimal LQG compensators for reduced-order control design. *Proceedings of the American Control Conference*, Baltimore, MD, June 1994; 3411–3415.
14. Ganesh C, Pearson JB. $\mathcal{H}_2$-optimization with stable controllers. *Automatica* 1989; **25**: 629–634.